According to Figure 1, the power is high when the group point of the simultaneous administration group is within the triangular region and the power is low when it is located outside that region. Consequently, the design to evaluate synergism should have the group point within the triangle region. Figure 2 shows the power reaches a peak near the boundary of the triangular region and decreases apart from the triangular region as the dose increases. In consequence, the group point should be located on the boundary of triangle region. Finally, according to Figure 3, the power achieves the steady state on the boundary of the triangular region and reaches a peak slightly outside the triangular region when Δ becomes larger linearly as the dose increases. In numerical example, recommended group point in Cases 1–3 is, respectively, $(d_A, d_B) = (0.6, 0.6), (0.9, 0.9), (1.4, 1.4)$ and the power is 81.4%, 80.4%, 88.4%, respectively.

The sensitivity analysis was conducted to investigate the usefulness of location of the group point in the real study, such as two group points $(d_A, d_B) = (0.5, 0.5)$ and $(1.0, 1.0)$. In this section, only group points for simultaneous administration were changed in the following way and all other conditions were the same.

4.2.3. Group points for simultaneous administration.

(1) $(d_A, d_B) = (0.6, 0.6)$ (recommended in Case 1)
(2) $(d_A, d_B) = (0.9, 0.9)$ (recommended in Case 2)
(3) $(d_A, d_B) = (1.4, 1.4)$ (recommended in Case 3)
(4) $(d_A, d_B) = (1.0, 1.0)$ (on the boundary)
(5) $(d_A, d_B) = (0.5, 0.5), (1.0, 1.0)$ (real study)

Here, the total sample size for simultaneous administration groups is fixed in all group points (1)–(5). Then n_m for two groups' simultaneous design such as (5) is half of that for one group's design.

The numerical calculation was conducted under the above conditions. Table 2 summarizes the reduction of power from a recommended group point. When the group point is located close to the boundary of the triangular region, the reductions of power from a recommended group point are small. Furthermore, in the situation of real studies, the loss of power is negligible compared to that in a recommended group point. It is considered that the configuration of the group points in real study is reasonable from the statistical viewpoint.

4.3. Recommended group size

In this section, under conditions in which the total number of animals is fixed and the effect sizes are varied, we investigate the group size of the simultaneous administration group that maximizes the power.

Table 2. Reduction of power from a recommended group point in three cases

Group point (d_A, d_B)	Case 1 (constant case)	Case 2 (square root case)	Case 3 (linear case)
(0.6, 0.6)	0.0	−10.2	−34.7
(0.9, 0,9)	−7.3	0.0	−9.3
(1.4, 1.4)	−34.6	−9.7	0.0
(1.0, 1.0)	−12.2	−0.4	−5.1
(0.5, 0.5), (1.0, 1.0)	−2.0	−2.6	−19.7

n_m for two group points is half of that for one group.

DOI: 10.1002/env

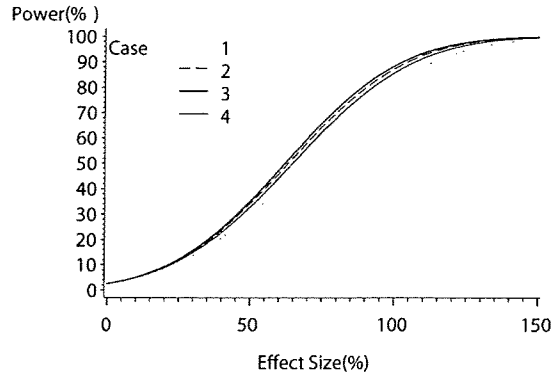

Figure 4. Relation between power and group size in four cases

4.3.1. Fixed conditions.

1. Group points for single administration: $(d_A, d_B) = (0, 0), (1, 0), (2, 0), (0, 1), (0, 2)$.
2. Group point for simultaneous administration: $(d_A, d_B) = (0.6, 0.6)$.
3. Parameters in the dose–response curve: $\beta_0 = 1.0$, $\beta_A = 1.0$, $\beta_B = 1.0$.
4. Variance σ^2: $\sigma_s^2 = \sigma_m^2 = 1.0$.
5. Nominal significance level of t-test: one-sided 2.5%.
6. Total number of animals: $n = 42$.

4.3.2. Varied conditions.

7. Group size:
   Case 1: $n_s = 6$, $n_m = 12$
   Case 2: $n_s = 5$, $n_m = 17$
   Case 3: $n_s = 4$, $n_m = 22$
   Case 4: $n_s = 3$, $n_m = 27$
8. Effect Size: $\Delta/\sigma_m = 0.1(0.1)1.5$.

Figure 4 shows the results of the numerical calculations, with the power on the vertical axis and the effect size on the horizontal axis. According to Figure 4, regardless of the effect size, Case 3 gives the maximum power. Because the group size is constrained to be an integer, it is not possible to give the most appropriate group size as a continuous value. The power becomes larger when the group size of the simultaneous administration group is set larger than that of the single administration group. When $n = 42$, what is prominent is the fact that the group size of 22 in the simultaneous administration group is nearly equal to the total number of animals in the single administration group, $4 \times 5 = 20$.

5. DISCUSSION

5.1. Conclusion under assumed conditions

In the previous section, we investigated applicable designs assuming that the response variables follow a homoscedastic normal distribution, that the dose–response relationship for single administration is

DOI: 10.1002/env

linear, that synergism is defined as a larger response obtained with simultaneous administration as compared to the dose plane obtained with single administration by assuming additivity, that there are five groups for single administration and one group for simultaneous administration, etc.

As the results of numerical calculation for the group point, when the departure Δ from additivity is proportional to square root of the dose, it is revealed that the group point for the simultaneous administration group should be on the boundary of the triangle region. Here, the results seemed to be reasonable. Because it is natural to expect that the departure Δ does not continue to increase along with the dose constantly. So, we applied these two situations as the sensitivity analysis. When the departure Δ become larger linearly along with the dose, the group point should be located slightly outside the triangle region. On the other hand, the group point should be set inside the triangle region when the departure Δ is constant. However, the group point should be placed on the boundary of the triangular region, because the reduction of power from a recommended group point is small. This means that the conventional design in the real study is appropriate.

Subsequently, with respect to the group size, we revealed that the total number of animals allocated to the simultaneous administration group should be same size as that in the single administration group.

5.2. *Heteroscedasticity*

When heteroscedasticity in data is expected from the past research, it is required to adjust the degree of freedom by using the Welch test. For the cases discussed in this paper, we used the Welch test, which is robust for heteroscedasticity because there is a tendency in real data for the variance to increase with an increase in responses although the number of animals is small. However, the Welch test does not control a type 1 error below the nominal significance level under heteroscedasticity. It is, therefore, required to confirm, *ex post facto*, the type 1 error when the degree of heteroscedasticity is large.

5.3. *Linearity*

For the cases discussed in this paper, based on advanced information, it was possible to select the dose so that there is linearity with the single administration group. This was easier due to the fact that the number of dose levels in the single administration group was small (three levels). From the experimental results, it was also confirmed that the linearity assumptions were established to some extent. When using the results in this paper, it is important to confirm the dose–response relationship in preliminary experiments or in past experiments using analogous substances. It is necessary to examine, *ex post facto*, the linearity by displaying in figure or by linearity tests.

5.4. *Group size*

The group size must be an integer of at least 1. In addition, the total number of animals must be a comparatively small. Under these conditions, as in this paper, it is necessary to obtain the appropriate design using numerical calculations, separately considering a combination of possible group sizes. However, in order to generalize these results, it is useful to perform power calculations, taking the group size as a continuous value. When calculating the recommended ratio of the total number of animals in the single administration group to the group size of the simultaneous administration group, the results shown in Figure 5 are obtained.

When determining the appropriate group point of the simultaneous administration group, with the departure Δ from the additivity being constant, the highest power is obtained by setting the number of

DOI: 10.1002/env

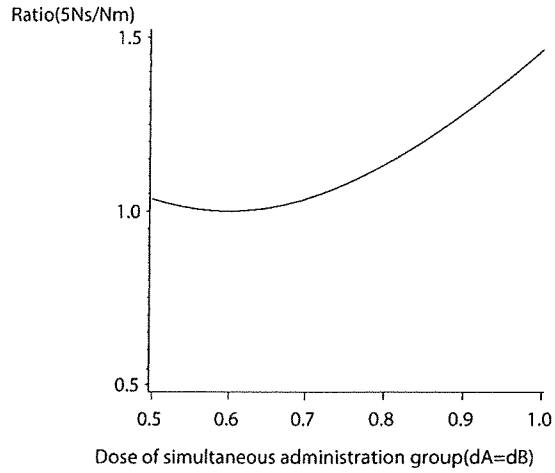

Figure 5. Recommended ratio of the group size between single administration group and simultaneous administration group

animals at a ratio of 1:1 between the single administration group and the simultaneous administration group.

When determining the simultaneous administration group on the boundary of the triangular region, a theoretical calculation shows that the allocation at a ratio of 1.464:1 is appropriate. In other words, it is best to set the total number of animals in the single administration group to be approximately 1.5 times the total number of animals in the simultaneous administration group. The reason is that because it is theoretically favorable for the accuracy of estimates based on additivity to be equal to that based on simultaneous administration.

5.5. Practical consideration on the recommended design

In the numerical examples of the previous section, we showed that the group point for the simultaneous administration on the boundary of the triangular region is not necessarily best and the recommended number of animals for the simultaneous administration group is considerably greater than those for single administration groups.

Although these results speciously imply that the design exemplified in the Subsection 4.1 should be replaced with the recommended design shown in this paper in future, we think it is not always true, because we have to take practical conditions into consideration, which were not incorporated in the assumptions to derive the recommended design.

One of them is the robustness or stability of the result of data analysis in such experiments. The situation is quite similar to that for the recommended design at linear regression analysis, for example, related to a single chemical experiment. Actually, if we can entirely assume the linearity of the dose–response relationship in regression analysis, the recommended design is to allocate a half of animals to the maximum dose and the remaining half to the minimum dose, while such design is really not adopted and animals are evenly allocated to uniformly distributed three or four doses probably to secure the robustness of the result of data analysis. Likewise, when the functional relationship of the Δ is not particularly clear, or when there is concern for the instability in squeezing the simultaneous administration group into one group in our experiments, the design with two or three simultaneous

DOI: 10.1002/env

administration groups within the triangular region must be practical. Since the mathematical formulation in such condition could not be established up to present due to its difficult nature, we left it for future investigation.

5.6. Other issues for future investigation

When the number of test substances is 3 or more, there needs to be strict controls for the number of required animals. Therefore, a design must be determined by examining the design conditions in detail for each case. Under this condition, an investigation following the same approach as in this paper is necessary. This is another problem to be addressed in future research.

In this paper, we introduced a test statistic by using the unweighted least squares method. The weighted least squares method must be considered when the rules for the size of variance are understood from past research, such that variance linearly becomes larger along with the dose. The specific design in this instance is also to be investigated in the future.

ACKNOWLEDGMENT

We thank Professor Takashi Sozu at Osaka University for his assistance in the preparation of this paper. We are grateful to the Editor-in-Chief and two anonymous reviewers for their comments that greatly improved this paper.

REFERENCES

Abdelbasit KM, Plackett RL. 1982. Experimental design for joint action. *Biometrics* **38**: 171–179.

Berenbaum MC. 1989. What is synergy? *Pharmacological Review* **41**: 93–141.

Gennings C, Schwartz P, Carter WH, Simmons JE. 1997. Detection of departures from additivity in mixtures of many chemicals with a threshold model. *Journal of Agricultural, Biological, and Environmental Statistics* **2**: 198–211.

Gennings C, Carter WH. 1995. Utilizing concentration-response data from individual components to detect statistically significant departures from additivity in chemical mixture. *Biometrics* **51**: 1264–1277.

Hasegawa R, Yoshimura I, Imaida K, Ito N, Shirai T. 1996. Analysis of synergism in hepatocarcinogenesis based on preneoplastic foci induction by 10 heterocyclic amines in the rat. *Japanese Journal of Cancer Research* **87**: 1125–1133.

Hewlett PS, Plackett RL. 1959. A unified theory for quantal response to mixtures of drugs: noninteractive action. *Biometrics* **15**: 591–610.

Kanno J, Onyon L, Haseman J, Fenner-Crisp P, Axhby J, Owens W. 2001. The OECD program to validate the rat uterotrophic bioassay to screen compounds for *in vivo* estrogenic response: phase 1. *Environmental Health Perspectives* **109**: 785–794.

Kelly C, Rice J. 1990. Monotone smoothing with application to dose-response curve and the assessment of synergism. *Biometrics* **46**: 1071–1085.

Laska EM, Meisner MJ. 1989. Testing whether an identified treatment is best. *Biometrics* **45**: 1139–1151.

Matsunaga N, Kanno J, Yoshimura I. 2003. A statistical method for judging synergism application to an endocrine disruptor animal experiment. *Environmetrics* **14**: 213–222.

Machado SG, Robinson GA. 1994. A direct, general approach based on isobologram for assessing the joint action of drugs in pre-clinical experiment. *Statistics in Medicine* **13**: 2289–2309.

Roy P, Esteve J. 1998. Using relative risk models for estimating synergy between two risk factors. *Statistics in Medicine* **17**: 1357–1373.

Straetemans R, O'Brien T, Wouters L, Dun JV, Janicot M, Bijnens L, Burzykowski T, Aerts M. 2005. Design and analysis of drug combination experiments. *Biometrical Journal* **47**: 299–308.

Tan M, Fang HB, Tian GL, Houghton PJ. 2003. Experimental design and sample size determination for testing synergism in drug combination studies based on uniform measures. *Statistics in Medicine* **22**: 2091–2100.

BIOCHEMICAL PHARMACOLOGY 77 (2009) 521–535

available at www.sciencedirect.com

ScienceDirect

journal homepage: www.elsevier.com/locate/biochempharm

Review

Aryl hydrocarbon receptor biology and xenobiotic responses in hematopoietic progenitor cells

Yoko Hirabayashi [a], *Tohru Inoue* [b,*]

[a] *Cellular and Molecular Toxicology Division, Center for Biological Safety and Research, National Institute of Health Sciences, Tokyo 158-8501, Japan*

[b] *Center for Biological Safety and Research, National Institute of Health Sciences, 1-18-1 Kamiyohga, Setagayaku, Tokyo 158-8501, Japan*

ARTICLE INFO

Article history:
Received 31 July 2008
Accepted 19 September 2008

Keywords:
Aryl hydrocarbon receptor
Hematopoietic stem/progenitor cells
Thioredoxin
Benzene
Gompertzean expressions

ABSTRACT

Studying the biological functions of the aryl hydrocarbon receptor (AhR) other than its function in xenobiotic drug metabolism may answer the questions as to why AhR orthologues have long been conserved phylogenically widely in the animal kingdom, and why homologues have diverged from nonvertebrate species such as nematodes and drosophila to all the vertebrate species. In this review, we focused on the mechanism of longevity possibly derived from evolution of AhRs and compared the functional difference of hematopoietic progenitors between wild-type ($AhR^{+/+}$) mice and AhR-deficiencies ($AhR^{+/-}$, $AhR^{-/-}$). Particular advantages found in wild-type mice compared with AhR-deficiencies were as follows: first, higher antioxidative function in the hematopoietic microenvironment with low oxidative tension seemed to have developed with the evolution of AhR; second, primitive hematopoietic progenitor-cell-specific deceleration and dormancy of cell-cycle regulation may have developed also with AhR evolution, which keeps hematopoietic progenitor cell compartment dormant without extinction by continuous differentiation; third, the consequent evolution of genomic stabilization with a longer lifespan in wild-type mice developed with the evolution of AhR. Experimentally, mice showed a significant extension of lifespan in a gene-dosage-dependent manner with a delayed onset of leukemogenicity. Another possible additional advantage observed in wild-type mice, the mechanism of which is not yet clarified, is an improved efficiency of fertilization in wild-type mice as compared with AhR-deficiencies, which seems to have developed with the evolution of AhR. Four advantages altogether, including the anti-aging feature mentioned above may have induced the AhR molecule to diverge various of species in the animal kingdom.

* *Corresponding author.* Tel.: +81 3 3700 1564; fax: +81 3 3700 1622.
E-mail address: tohru@nihs.go.jp (T. Inoue).

Abbreviations: AhRs, aryl hydrocarbon receptors; ARNT, aryl hydrocarbon receptor nuclear translocator; BM, bone marrow; BrdUrd, 5-bromo-2′-deoxyuridine (RN: 59-14-3); CFU, colony forming unit; CFU-E, colony forming unit-erythroid; CFU-GM, colony forming unit-granulocyte macrophage; CFU-S, colony forming unit in spleen; CYP, cytochrome P450; DCFH-DA, 2′,7′-dichlorodihydrofluorescein diacetate; Hif, hypoxia-inducing factor; KO, knockout; LKS fraction, a hematopoietic progenitor fraction with stem cell antigen (Sca1) and c-kit, without surface lineage-restricted antigen; MNU, 1-methyl-1-nitrosourea (RN: 684-93-5); PAS, the *Drosophila* period clock protein (PER), vertebrate ARNT, and *Drosophila* single-minded protein (SIM); PLTs, platelets; RBCs, red blood cells; ROS, reactive oxygen species; TCDD, 2,3,7,8-tetrachlorodibenzo-*p*-dioxin (RN: 1746-01-6); UV, ultraviolet; WBCs, white blood cells; XRE, xenobiotic responsive element.

0006-2952/$ – see front matter
doi:10.1016/j.bcp.2008.09.030

Contents

1. Introduction—The hematopoietic stem cells and aging as a xenobiotic tissue model

The aryl hydrocarbon receptor (AhR) is a xenobiotic receptor, which plays a role as a transcriptional master molecule for drug-metabolizing enzyme genes and protooncogenes after binding to their xenobiotic responsive element (XRE) [1–3]. An orthologue of the gene was identified not only in vertebrates but also in invertebrates; however, xenobiotic ligands such as 2,3,7,8-tetrachlorodibenzo-*p*-dioxin (TCDD) are not bound in invertebrates [4]. Although the functions of AhR in invertebrates are considered to be different from those in vertebrates, the function of AhR in vertebrates is considered to have biological commonalities other than xenobiotic responses, which is focused on in this review article.

To elucidate the biological functions of AhR, it may be strategically worthwhile to analyze tissue stem cells as a model because the expression level of AhR tends to show a graded decrease along the course of stem cell differentiation [5]. Tissue-specific responses to oxidative stress via AhR [6] are consequently attenuated along the course of stem cell differentiation. Specifically, hematopoietic stem cells are the focus of many studies such as the induction of genomic instability along a graded increase in oxidative stress due to xenobiotic metabolism, and the consequent deletion of telomere length, increase or decrease in telomerase activity, along with the cascading changes of shortening of cellular senescence, development of cancers, broadening of the noncarcinogenic disease spectrum, and consequent shortening of life [7].

In this introduction, an overview on hematopoietic stem cell physiology and alteration of senescence is discussed because physiological and xenobiotic functions of AhR are discussed in this chapter focusing on the hematopoietic system.

Hematopoietic stem cells were discovered half a century ago when development of hematopoietic spleen colonies derived from shielded bone marrow was discovered after whole-body radiation exposure of mice to a lethal dose [8].

In 1961, Till and McCulloch observed spleen colonies in recipient mice a week after lethal-dose radiation exposure followed by injection of intact bone marrow cells [9]. The progenitors of these spleen colonies were named spleen colony forming units (CFU-S), whose progeny and clonal growth were subsequently discovered [10]. Five years after the discovery of CFU-S, in vitro formation of colonies that are also derived from relatively matured hematopoietic progenitor cells was discovered by Pluznik and Sachs [11], and Bradley and Metcalf [12], simultaneously in 1965, which are called CFUs in culture. Continuous bone marrow transplantation with biological markers led to the idea that the progenitors of these CFUs are nearly infinite at that time [13]. The hierarchical generation-age structure from these hematopoietic progenitor cells to differentiated red blood cells (RBCs), polymorphic white blood cells (WBCs) via intermittent committed progenitor cells was developed by later series of studies along with development of biological differentiation cellular markers [14,15]; currently, the lineage-negative, c-kit-positive, stem cell antigen (Sca)-1-positive (LKS) cellular compartment is used in experiments as practically most primitive hematopoietic progenitor cells [16,17].

The senescence of hematopoietic progenitor cells was studied in the early 70 using W(c-kit) mutant mice as recipients focusing on the long-term sustainability of recipients as well as on the long-term repopulation after continuous marrow transplantation. Continuous bone marrow transplantation showed continuous clonal survivors of the first generation of bone marrow cells for up to one hundred months [13]. However, the correct number of generation times during that time was not countable, implying that progenitor

cells are capable of infinite growth but show decreased growth rate with age, probably because there is only a slight decrease in the telomere length of the hematopoietic stem cell compartment. The telomerase-deficient mice established by DePinho et al., which lack the essential RNA component for telomerase haloenzyme, interestingly showed a decreased life span as continuously observed for six generations [18], which provides another piece of evidence that hematopoietic progenitor cells possess a nearly infinite growth potential.

Concerning the role of hematopoietic stem cells during aging in an individual, an early onset of spontaneous as well as induced leukemias are observed in p53-deficient mice owing to impaired cyclin-dependent kinase inhibitors after chemical- and radiation-induced injuries. Hematopoietic "niches" are thought to contain genes, such as N-cadherin [19–21], Jagged1/Notch [22], Ang1/Tie-2 [23], osteopontin [24], and SDF1(CXCL12)/CXCR4 genes [25,26]. Cellular senescence of hematopoietic progenitor cells in vivo is also related to stem cell settlements of the hematopoietic microenvironment called niches where primitive hematopoietic progenitor cells locate beneath the epiphyseal bone matrix of the bone marrow. In addition, although it is still speculative, connexin (Cx) 32 molecules were firstly found to be localized solely in primitive hematopoietic stem cells. Thus, they are supposed to be an important component of niches; however, interestingly, methyl nitrosourea (MNU)-induced leukemias develop more preferentially when the Cx32 molecules are deficient [17,27]. It is of interest to clarify the mechanism underlying genomic instability possibly available in Cx32-impaired hematopoietic niche.

Hematopoietic stem cells can be a target of xenobiotic effects; this possibility is not hypothetical but remains limited [28]. Ionizing radiation of p53-deficient mice induces leukemias, which are characterized by stem cell leukemia [29]. The mechanism underlying the development of stem cell leukemia following ionizing radiation is considered to be based on the function of p53, which is required for stem cell differentiation [30].

Concerning the development of lymphoid stem cell lineages, lymphopoiesis also depends on hematopoietic progenitor cell function [31]. Similarly to steady-state hematopoiesis, supported by hematopoietic niches and stromal cells as the source for hematopoietic regulatory cytokine expression, hematopoiesis cannot occur without hematopoietic stromal elements [32]. Hematopoietic stromal cells support hematopoiesis by at least two pathways: one for cell-to-cell interaction [33] and the other for positive and negative cytokine regulations. In the case of B lymphocyte progenitor cells, it was found in stromal-cell-impaired mutant mice, SAM/P1, that B lymphopoiesis is impaired during senescence owing to the simultaneous decrease in the expression levels of positive regulator IL-7 and the negative regulator TGF-beta, which Tsuboi [34] called vicious suppressive homeostasis during senescence.

2. Aryl hydrocarbon receptor and its evolutional driving forces

AhR was found to be a ligand-activated transcriptional factor with halogenated ligands such as TCDD; however, the ligand-specific activation was found only in vertebrates. Nevertheless, conservation of diverse homologues across vertebrate species suggests common physiological functions across species [4,35]. What was its original function? In this section, mechanisms underlying phylogenic development of AhR, i.e., possibly based on physiological advantages of AhR, are reviewed.

2.1. *Aryl hydrocarbon receptor and phylogenic development*

AhR is a member of the basic helix-loop-helix/PER-aryl hydrocarbon receptor nuclear translocator (ARNT)-SIM (bHLH-PAS) family, which consists of transcriptional regulatory proteins [1,2] whose cDNA was cloned by Ema et al. [36] and Burbach et al. [37], and the gene was characterized by Schmidt et al. in 1993 [38]. Since then, a number of homologues of AhR in mammalian species; such the human species (*Homo Sapiens*) [39], various mice (*Mus musculus*) [36,37,40,41], rats (*Rattus norvegicus*; Sprague–Dawley [42], Han-Wistar [43]), hamster (*Mesocrisetus auratus*) [44], Atlantic white-sided dolphin (*Lagenorhynchus acutus*) [4], and Baikal seal (*Phoca sibirica*) [45], were cloned. Moreover, nonmammalian vertebrates, such as birds [4,46,47], amphibians [47], bony fishes [4,48–52], cartilaginous fishes [35,53], lampreys (*Petromyzon marinus*) [4,53], and invertebrates such as soft-shell clam (*Mya arenaria*) [54], zebra mussel (*Dreissena polymorpha*) [4], nematode (*Caenorhabditis elegans*) [53], and fruitflies (*Drosophila melanogaster*) [55], were cloned.

According to Hahn in 2002 [4], the ability of AhR to bind halogenated ligands and mediate an adaptive response involving induction of xenobiotic metabolizing enzymes may have been a vertebrate's innovation because invertebrate AhRs were reported to not bind to those ligands. Therefore, the physiological functions of AhR may be initiated from invertebrate species. Those functions mediated by an AhR orthologue in invertebrates are, reported to not bind to TCDD and other synthetic AhR ligands; thus, they are distinguished from those in vertebrates. Furthermore, their functions are found to be necessary for development of distal segments of the antennae and legs [55,56], and further for the specification of photoreceptor identity in the retina [57] in a *Drosophila* AhR homologue, spineless, and for the expression of *C. elegans* ahr-1 in sensory neurons in regulation of neuronal differentiation [58,59]. However, our knowledge on invertebrates may be insufficient to draw general conclusions between AhRs expressed in vertebrates and in invertebrates, but those functions are seemingly not comparable to each other because while those expressed in vertebrates are largely in cycling cells, the others expressed in invertebrates are not in cycling cells but in postmitotic cells. In the case of the PAS domain, it is far more widely distributed from animals to plants, fungi, bacteria, and Archea, its functional evolution does not seem to parallel its molecular evolution. Is there any common functional evolution across vertebrate species?

2.2. *Physiological function of aryl hydrocarbon receptor: Advantages in fertility?*

It may not be the right answer to the question; however, we found that our knockout mice, both homozygous and

Table 1 – Reproductive toxicology in AhR-deficiencies.

Genotype of parents		No. of pups (sets[a])	Sex		Genotype		
Mother	Father		Male	Female	+/+	+/−	−/−
			(Genotype: $AhR^{+/+}$, $^{+/-}$, $^{-/-}$)		(Sex: male, female)		
AhR+/+	AhR+/−	154 (18)	71 (46, 25, –)	83 (50, 33, –)	96 (46, 50)	58 (25, 33)	– (–, –)
AhR+/−	AhR+/−	206 (27)	100 (36, 48, 16)	106 (32, 53, 21)	68 (36, 32)	101 (48, 53)	37 (16, 22)

[a] Sets for mating: each set consists of 2 females and 1 male.

hemizygous males, show a greater dysfunction in fertilization than wild-type male mice. For example, during reproduction in the current generation, crossbreeding between hemizygous AhR-knockout (KO) male mice and wild-type female mice produced 71 males and 83 females (Table 1). Among these, 96 mice were of the wild type and 58 mice were hemizygous AhR-KO. Although the number of puppies of wild-type mice and that of hemizygous AhR-KO mice were supposed to be equal in accordance with the Mendelian law, the number of puppies of hemizygous AhR-KO mice (58) was 60.4% lower than that of wild-type mice (96). Interestingly, this low incidence seemed to be largely based on the hemizygous AhR-KO males, because, among the 71 male puppies mentioned above, 25 were hemizygous AhR-KO mice, and 46 were of the wild type, which showed a statistically significant difference ($p < 0.028$). Among the 83 puppies mentioned above, 33 puppies were female hemizygous AhR-KO mice and 50 female puppies were of the wild type, which showed a statistically insignificant difference ($p > 0.064$). Furthermore, the mating study disclosed a more detailed underlying mechanistic background of reproductive dysfunction in male AhR-KO mice. When hemizygous AhR-KO males and their corresponding females were crossbred, the numbers of puppies observed were 100 males and 106 females (Table 1). Among them, the numbers of puppies were 37 homozygous AhR-KO mice, 101 hemizygous AhR-KO mice, and 68 wild-type mice. Because the average number of puppies of C57BL/6 mice at the animal colony was 6–7 mice per litter, the number of puppies observed in the present study was slightly larger than this average (132%), that is, 51.5 puppies, calculated from the total number of puppies (206) divided by 4 (25%) on the basis of the Mendelian law. These results imply that the incidence of homozygous AhR-KO mice was 45.6% lower than the incidence expected from the Mendelian law. Furthermore, this lower incidence is not supposed to be due to the death of AhR-KO puppies; but rather, AhR-KO puppies were supposed to have shifted to the wild type, because the cross-breeding was between hemizygous AhR-KO mice, in which sperms derived from the testicular glands of AhR-KO and wild-type may have competed during fertilization for fertilizing function. Indeed, when homozygous AhR-KO mice were crossbred, neither their litter size nor the ratio of the number of males to that of females was statistically significantly different from that of the wild type, because the competitive disadvantages observed in the hemizygous AhR-KO mice may have been negated by the same testicular dysfunctions in the homozygous AhR-KO mice. The underlying mechanism of the testicular dysfunction is remained to be undetermined. Weight of the testes in AhR-KO mice is generally smaller than those in wild-type mice (75.2 ± 4.2, 84.9 ± 8.1, 105.5 ± 1.4 mg; homozygous AhR-KO, hemizygous AhR-KO, and wild-type mice, respectively). Possible fictional differences of their testicular glands may be more evident in AhR-KO mice treated with MNU (50 mg/kg body weight) than in nontreated mice. The testicular body ratio after MNU treatment in wild-type mice show a 91.0% decrease in wild-type mice compared with the control without MNU treatment, whereas the ratio after MNU treatment in AhR-KO mice show a 71.4% decrease compared with the same control wild-type mice without MNU treatment. These results indicate that the testicular tissue of AhR-KO mice shows a dysfunction in cellular proliferation and regeneration during the course of the development and the recovery after tissue injury.

Nebert et al. also found a low fertility in the D2-linked DBA strain, which seems to be linked to AhR affinity [60]. Thus, AhR seems to contribute to the stabilization of fertilization, which might be one of the reasons its gene has diversified across species during the course of its evolution. Because the focus of this section is the hematopoietic system, further description on the functional contribution of AhR to fertilization may be discussed elsewhere.

2.3. $AhR^{-/-}$ mice show earlier onset of spontaneous neoplasms—Gompertzean accelerated aging

Fig. 1 shows the incidence of spontaneous malignant lymphomas in each genotype group for AhR plotted along the ordinate axis vs. age in days plotted along the horizontal axis. The development of lymphomas in the $AhR^{-/-}$ group (darkly shaded columns) starts earlier than that in the $AhR^{+/-}$ (lightly shaded columns) and wild-type (open columns) groups. The incidence

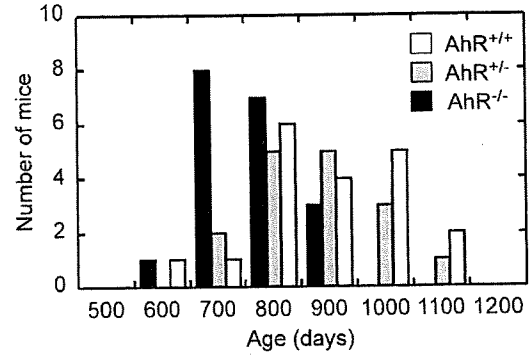

Fig. 1 – Incidences of spontaneous malignant lymphomas at unit time intervals for wild-type ($AhR^{+/+}$) mice and AhR-deficient ($AhR^{-/-}$, $AhR^{+/-}$) mice. (Open columns, $AhR^{+/+}$; lightly shaded columns, $AhR^{+/-}$; darkly shaded columns, $AhR^{-/-}$ groups.)

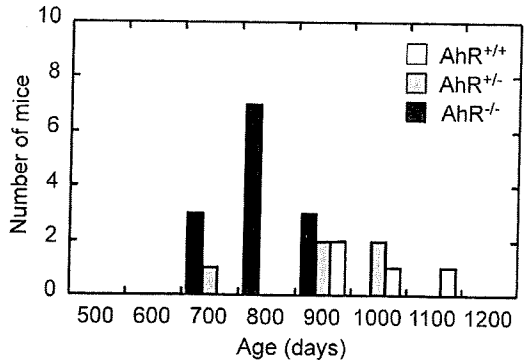

Fig. 2 – Incidences of spontaneous hepatomas at unit time intervals in wild-type ($AhR^{+/+}$) mice and AhR-deficient ($AhR^{-/-}$, $AhR^{+/-}$) mice. (Open columns, $AhR^{+/+}$; lightly shaded columns, $AhR^{+/-}$; darkly shaded columns, $AhR^{-/-}$ groups.)

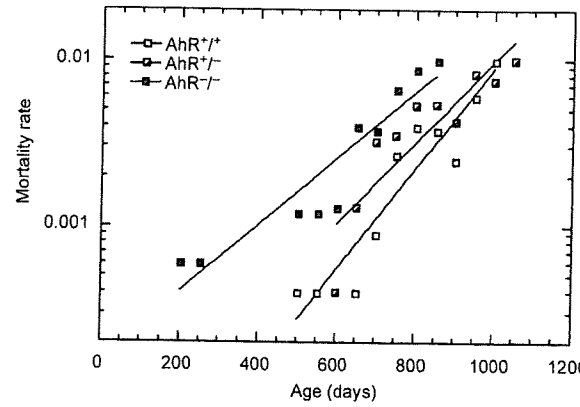

Fig. 3 – Gompertzean expressions [61] of mortality rates of mice of different genotypes: wild-type ($AhR^{+/+}$) mice and AhR-deficient ($AhR^{-/-}$, $AhR^{+/-}$). (Open squares, $AhR^{+/+}$; half-closed squares, $AhR^{+/-}$; closed squares, $AhR^{-/-}$ groups.)

of lymphomas in the $AhR^{-/-}$group peaked at 700 days old, whereas those in the $AhR^{+/-}$ and wild-type groups peaked at 850 and 1000 days old, respectively. Similarly, the incidences of spontaneous hepatomas in each genotype group are plotted in Fig. 2. In this figure, spontaneous hepatomas in the $AhR^{-/-}$ group appear at 700 days old and those in the wild-type group appear much later (900 days) at significantly lower incidences. In Fig. 3, the mortality rate/unit time interval for each genotype group is plotted. Mortality rate/unit time interval is shown in the ordinate on a logarithmic scale and age in days is plotted along the horizontal scale (Gompertzean expression [61]). In this figure, the line for closed squares for the $AhR^{-/-}$ mice shows a much early onset curve with a lower and flatter slope than the line for open square for the wild-type group. Thus, the mortality rate of the $AhR^{-/-}$ group can be concluded to indicate "accelerated aging". The shortened lifespan observed in the AhR-KO mice may be due to the impairment of a possible suppression gene in the KO mice. However, some mice for each survival curve are non-tumor-bearing mice. The mechanism of this accelerated aging may not be as simple as that involving a tumor suppressor and remains to be elucidated.

AhR is an orphan receptor whose original physiological function remains unclarified. Since AhR-KO mice were found to show an earlier onset of spontaneous neoplasms than wild-type mice, AhR was assumed to play a suppressor gene function [62]. However, because not all AhR-KO ($AhR^{-/-}$) mice or wild-type mice die of spontaneous neoplasms, the function of wild-type AhR may also be associated with a possible genomic stabilization, consequently extending the lifespan of mice simultaneously. What are the underlying mechanisms that contribute to the extended longevity? Evaluation of reactive oxygen species (ROS) using the 2′,7′-dichlorodihydrofluorescein diacetate (DCFH-DA) dye (Fig. 4) showed a prominent increase in oxidative stress in unfractionated bone marrow cells as well as in hematopoietic progenitor cells in AhR-KO mice [63] (Fig. 5). Hematopoietic progenitor cells are quiescent in anoxic environment, and are regulated by a weak oxidative stimulation as redox homeostatic regulation [64]. Thus, the reactivity of the fraction to the DCFH-DA dye was higher in AhR-KO mice than in wild-type mice, which is in good agreement with the mechanism underlying genomic stabilization under a

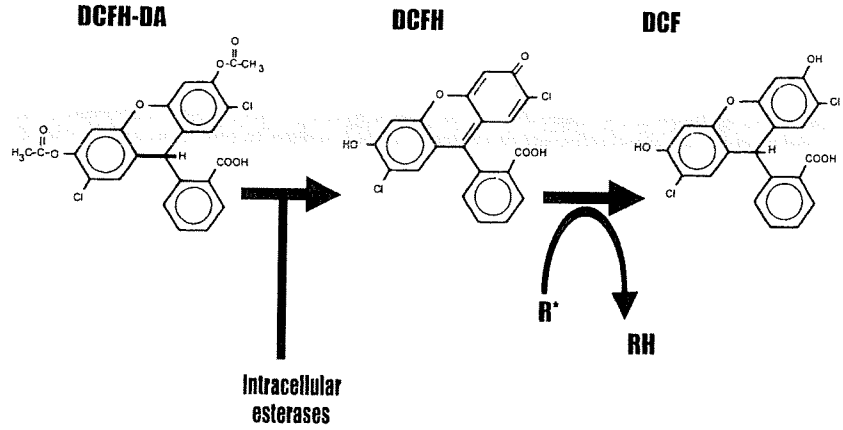

Fig. 4 – 2′,7′-Dichlorodihydrofluorescein diacetate (DCFH-DA) as ROS indicator [92] (DCFH: 2′,7′-dichlorodihydrofluorescein, DCF, 2′,7′-dichlorofluorescein).

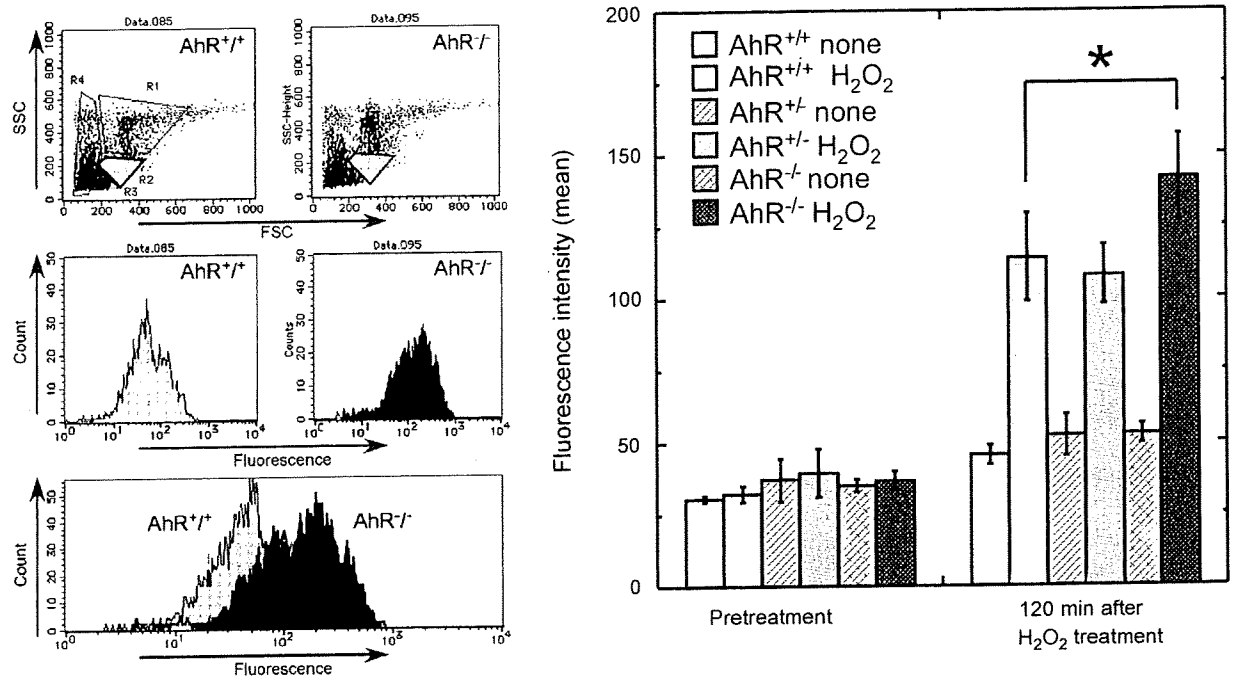

Fig. 5 – Fluorescence intensities of DCF dye in primitive bone-marrow cell fraction between the steady state (none) and the H_2O_2 treatment. Left panel, top row: primitive progenitor cell compartment (R2) were sorted out from bone marrow (BM) cells of wild-type ($AhR^{+/+}$) mice (left) and AhR-KO ($AhR^{-/-}$) mice (right) using a cell sorter as displayed between the forward scatter (horizontal axis) and the side scatter (ordinate axis). Left panel, middle and bottom rows: Relative cellular counts of the hematopoietic progenitor cells, ordinate axis vs. DCF dye-fluorescence intensity, horizontal axis, are compared between $AhR^{+/+}$ mice (middle left) and $AhR^{-/-}$ mice (middle right). Both profiles are compared in the bottom. Right panel: Fluorescence intensity of DCF dye of primitive hematopoietic progenitor fractions (R2 area) before (pre) and after (H_2O_2) treatment. Fluorescence intensity of DCF dye in R2: Groups for H_2O_2 treatment at 0 min on the left bars ($AhR^{+/+}$, none and H_2O_2; $AhR^{+/-}$, none and H_2O_2; $AhR^{-/-}$, none and H_2O_2, respectively), and Groups for H_2O_2 treatment at 120 min on the right bars ($AhR^{+/+}$, none and H_2O_2; $AhR^{+/-}$, none and H_2O_2; $AhR^{-/-}$, none and H_2O_2, respectively).

low oxidative tension in combination with the suppressor gene function and the consequent longevity observed in wild-type mice.

2.4. *Longevity as essential driving force for evolution of AhR*

Different mouse strains in terms of aryl hydrocarbon receptor function, receptor concentrations, and lifespans are compared. Because mice of different strains show different spontaneous neoplastic propensities, sometimes possess different AhR structures, and have different lifespans, available databases for such AhR-related functional parameters were compared. The results obtained are shown in Table 2.

In this table, two strains, namely, C3H/He and DBA/2, showed a low affinity or a low enzyme activity for constitutively activated cytochrome P450 (CYP) 1A2, whereas C57BL/6J, showed a high affinity or a high enzymatic activity for CYP1A2

Table 2 – AhR binding affinities and receptor activities, cell cycles, and life spans among murine species.

Strain	AhR affinity[a]	CYP1A2 enzyme activity[b]	Receptor concentration[c]	Cell cycle[d]	Lifespan[e] (days)	Notes
C3H/He	High	Low to mid	86 ± 23	High	500	Low signal induction
DBA/2J	Low	Low	–	High	710	708.7 days in other litr.[e]
C57BL/6J	High	High	151 ± 26	Low	789	860.8 days in other litr.[e]

[a] Murine Ah receptor specified by the Ah^d and Ah^{b-3} alleles is compared.
[b] Activities for methoxyresorufin o-demethylation (MOD) and pentoxyresorufin o-dealkylation, and metabolic activation of IQ for phenobarbital were tested. For activity in DBA/2J, high in male, but low in female for CYP1A2. Activity for MOD was significantly low for both genders [65].
[c] Murine Ah locus (mg/protein) [66].
[d] Scored using hematopoietic cobblestone area-forming cell assay [67].
[e] Data cited from Van Zant and de Haan [67] and Forster MJ et al. [68].

[65]. Although C3H/He mice showed a high affinity, the receptor concentration (mg/protein) measured was low [66]; thus, the total activity reported in the literature is low. It is interesting to determine correlations between AhR activity and the stage of cell cycle or lifespan, because mice with a high AhR activity, i.e., C57BL/6J, seem to show a suppressed cell cycle and longer lifespan, whereas mice with a low AhR activity, i.e., C3H/He, seem to show an accelerated cell cycle with a shortened lifespan [67,68]. No comparable data on genomic stability (or instability) fully supports the above-mentioned AhR activity are available. However, the correlations between AhR activity and the stage of cell cycle or lifespan seem to be plausible and compatible with the results of our present study of experimental induction of AhR-deficiencies.

We also found that AhR-KO mice show an earlier onset of spontaneous neoplasms than wild-type mice [62]. Thus, it is plausible that *AhR* functions as a tumor suppressor gene in the steady state. Furthermore, because not all of these mice die of malignant neoplasms, AhR may also extend the lifespan of these mice, i.e., it has "longevity" function (Fig. 6). Such biological plausible functions are possible reasons for the molecular evolution of *AhR* from homologues in invertebrates, such as nematodes, equivalent to those in vertebrates. However, one question remains: Why do AhR-KO mice show early onset of spontaneous neoplasms? Supposedly these mice should exhibit unfavorable xenobiotic responses when AhR is knocked out [69]. Furthermore, the mechanisms of the possible suppressive function of wild-type *AhR* remain to be elucidated.

Successful fertilization, tumor suppression, and longevity seem to be essential driving forces of phylogenic evolution of AhR in vertebrate species or, if not all, at least in mammalian species. Not many similar reports are available in the literature but some of them are strongly linked to the present issue. According to Abbott [70], the concentrations of AhR after birth increased rapidly and plateaued from 2 to 21 days and then rapidly decreased in the liver and lungs. Nebert et al. also discussed about the possible AhR-mediated longevity but the lifespan of experimental mice is too short to speculate on longevity [60]. This was supported by a study by Spindler et al. in 1989, which showed distinct differences in the maximum lifespan among different mouse strains with different induction levels of cytochrome p450s [71]. These previous studies suggest the functional advantages of AhR expression, but the mechanism underlying these functional advantages are poorly described. These are much strongly related to the localization of AhR expression in the tissue and AhR-mediated cell-cycle regulation. Findings possibly related to these issues will be described later.

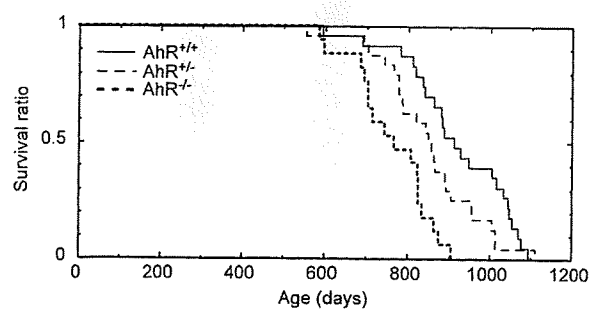

Fig. 6 – Survival curves for wild-type ($AhR^{+/+}$) mice and AhR-deficient ($AhR^{-/-}$, $AhR^{+/-}$) mice. (Solid line, $AhR^{+/+}$; long dotted line, $AhR^{+/-}$; short dotted line, $AhR^{-/-}$ groups.)

3. Hematopoietic progenitor cells and their cell-cycle regulation

As discussed in the previous section, although we know that AhR functions in maintaining lifespan, we do not know its underlying mechanism. In this particular section, we focus on the biological function of AhR in hematopoietic progenitor cells and in their cell-cycle regulation to elucidate the relevant mechanism that may explain such advantages of the function of AhR.

The hematopoietic microenvironment is hypoxic [72,73], which is located beneath the periosteal region and forms niches. The niches are thought to consist of genes, such as N-cadherin [19–21], Jagged1/Notch [22], Ang1/Tie-2 [23], osteopontin [24], and SDF1(CXCL12)/CXCR4 [25,26] genes, and possibly also the connexin 32 [17,27] gene, which maintains dormancy of hematopoietic stem/progenitor cells, because of the hypoxic state located distant from the vascular network. Stromal cells and endosteal cells in the hypoxic state may express hypoxia inducible factor (Hif)-1alpha [74], and also in some cases, HIF-2alpha [75] is expressed by hematopoietic stem/progenitor cells themselves, which may interact with ARNT molecules leading to steady-state hematopoiesis.

Regarding xenobiotic responses induced by AhR, hematopoiesis is often suppressed probably because of a possible recruitment of ARNT molecules to activate AhR. The monumental study by Luster in 1985 [76] showed a decrease in CFUs following the exposure of mice to TCDD, which may be based on this mechanism. AhR signaling also induces cell-cycle suppression, the mechanism of which has not been elucidated. Nevertheless, such deceleration of cell cycle in hematopoietic stem/progenitor cells contributes to longer stem cell survival, which may be the reason for the extension of animal lifespan.

3.1. *Aryl hydrocarbon receptor regulates hematopoietic progenitors*

When AhR is activated by xenobiotic ligands, ligand-specific transcription induces the production of drug-metabolizing enzymes, Cyp1A1 and 1B1, as the major products [1,2], which in turn induce oxidative stresses [6,77] and the consequent hematopoietic impairment by the up-regulation of cyclin-dependent kinase inhibitors [78,79]. Such hematopoietic impairment in stem-cell-specific cell cycling can be evaluated by the BUUV method [27,80], which is described in Section 3.3. Under xenobiotic stimulation with AhR ligands, a slight inhibition of transportation of ARNT required by Hif-1alpha and Hif-2alpha in the hypoxic hematopoietic microenvironment induces a possible inhibition of primitive hematopoiesis. On the other hand, steady-state expression of AhR makes ARNT available for Hif-1alpha and Hif-2alpha, the up-regulation of which is maintained by the relatively hypoxic hematopoietic microenvironment. Thus, AhR is important because ARNT released from AhR functions in transcription of

various hematopoietic factors, such as erythropoietin, CXCR4 [81], SDF-1 [73], vascular endothelial growth factor (VEGF) [82], and VE-cadherin [83]. According to the study by Adelman et al. on ARNT-KO mice, production of various CFUs derived from hematopoietic progenitors from embryonic stem (ES) cells markedly decreases in a ARNT-gene-dosage-dependent manner [84]. ARNT is, thus, important to maintain such primitive hematopoiesis.

3.2. *Aryl hydrocarbon receptors and cell cycle*

Whether AhR physiologically suppresses cell growth through relevant signals via a possible endogenous ligand [85] or facilitates cell-cycle progression from G_1 with *Fos* and *Jun* signaling, remains controversial [86]. In the authors' previous study, authors attempted to elucidate a possible hidden function of AhR in hematopoiesis using AhR-knockout mice [87].

3.2.1. *Aryl hydrocarbon receptor and B cell progenitors*

As the authors focused on B cell suppression during B lymphopoiesis [5], the effects of TCDD exposure on hemopoiesis were extensively investigated, since the inhibitory effects of TCDD on bone marrow and immunological parameters, including granulocyte-macrophage (GM) colony forming unit (CFU) and other progenitors, were first recognized by Luster and coworkers in the early 1980s [76,88]. The down-regulation of AhR expression attenuates myelosuppression in thioredoxin (Trx)-overexpressing mice, as determined by hemopoietic colonization assay, which elucidated the linkage of AhR signals to the antioxidant cascade induced by reactive oxygen species, ROS, after TCDD exposure [89,90].

In studies of Trx-overexpressing mice, attention was focused on the function of AhR in the hemopoietic system, specifically in hemopoietic stem cells/progenitor cells, and the controversial dual function of AhR was found to be consistent because AhR seems to stimulate the cell cycle as an early response to cytokines, whereas simultaneously, suppresses hematopoiesis during the steady state. The Janus-like dual function of AhR found in our present study may contribute to a better understanding of individual health effect that can be induced by an interaction between AhR and its environmental ligands.

3.2.2. *$AhR^{-/-}$ mouse shows significant enhancement of hematopoiesis*

The number of WBCs increases in $AhR^{-/-}$ mice (Fig. 7(a)). This is the first observation in $AhR^{-/-}$ mice [91] that is consistent with the hypothetical description by Adachi et al. [85] in which a possible physiological ligand is speculated to suppress hema-

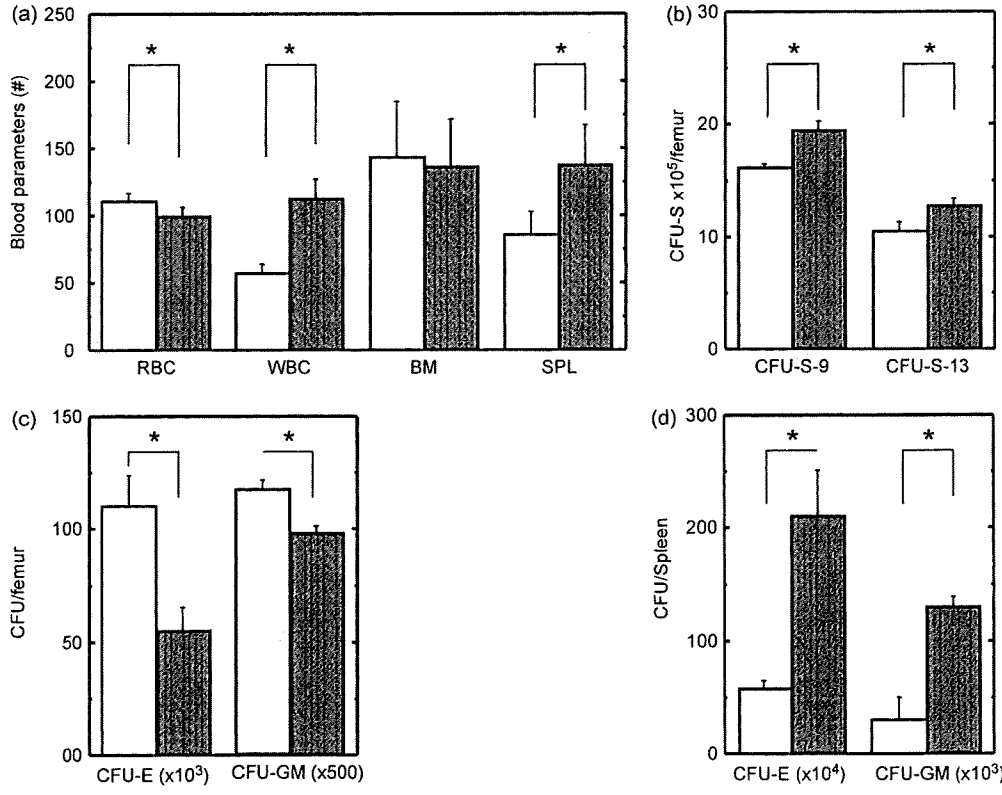

Fig. 7 – Comparison of various blood parameters between wild-type mice (open columns) and AhR-KO ($AhR^{-/-}$) mice (shaded columns); (a) peripheral blood, bone marrow (BM) and spleen weight. #: Vertical axis "Parameters" indicate the counts of peripheral red blood cells (RBCs, $\times 10^8$/ml) and white blood cells (WBCs, $\times 10^6$/ml), BM cellularity ($\times 10^5$/femur), and weight of the spleen (SPL, mg). (b) Number of colony forming units in spleen (CFU-S, $\times 10^5$/femur) observed on days 9 (CFU-S-9) and 13 (CFU-S-13). (c) Numbers of in vitro granulocyte-macrophage CFUs (CFU-GM, ×500/femur) and erythroid CFU (CFU-E, $\times 10^3$/femur) in femoral BM. (d) Numbers of CFU-GM ($\times 10^3$/spleen) and CFU-E ($\times 10^4$/spleen) in spleen.
***: Significant difference between wild-type and AhR-KO mice determined by t-test at $p < 0.05$.**

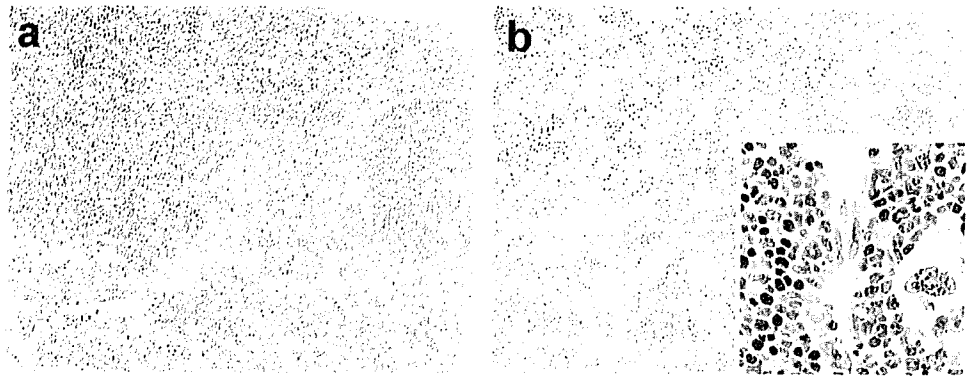

Fig. 8 – Histopathological findings in spleen from wild-type mice (a) and AhR-KO ($AhR^{-/-}$) mice (b). Note, a prominent enhancement of hemopoiesis in the spleen can be observed in $AhR^{-/-}$ mice (b). (HE staining. Magnification: a and b ×20, inset of b ×80.)

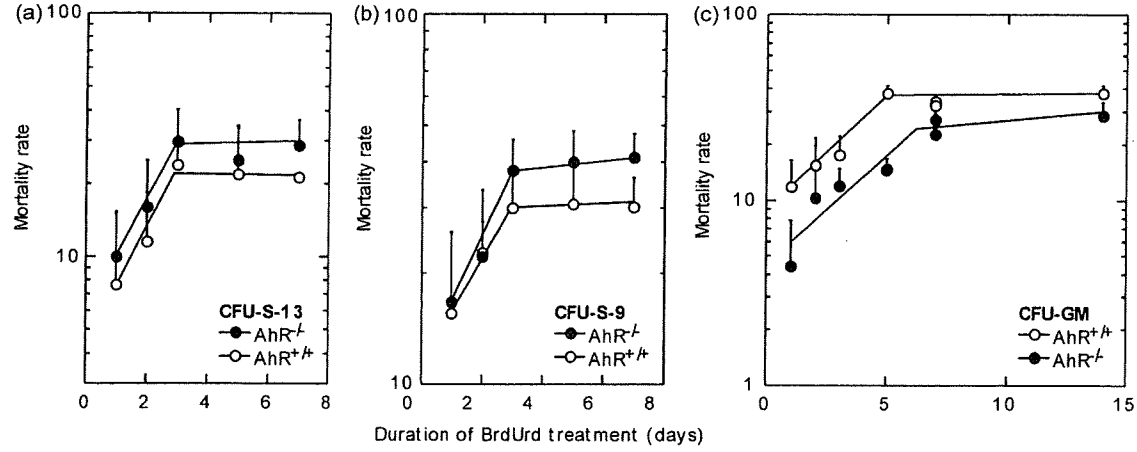

Fig. 9 – Hemopoietic progenitor cell kinetics of each hemopoietic progenitor compartment from wild-type mice ($AhR^{+/+}$) (open symbols) and AhR-KO ($AhR^{-/-}$) (closed symbols), measured by BUUV method [32,80]; numbers of colony forming units in spleen observed on days 13 (CFU-S-13) (a) and 9 (CFU-S-9) (b), and numbers of granulocyte-macrophage CFU (CFU-GM) (c). CFU-S-13 and CFU-GM are significantly different as determined by a paired t-test between $AhR^{+/+}$ and $AhR^{-/-}$ mice ($p < 0.05$). The plateau level (between day 3 and day 7 of BrdUrd treatment) of CFU-S-9 is also significantly different, as determined by the t-test between $AhR^{+/+}$ and $AhR^{-/-}$ mice ($p < 0.05$)).

topoiesis in $AhR^{+/+}$ mice. This is also consistent with the higher numbers of myeloid progenitor cells, i.e., CFU-S-9 and CFU-S-13, observed in $AhR^{-/-}$ mice (Fig. 7(b)). Thus, steady-state hematopoiesis is presumed to be suppressed via AhR signaling by a possible physiological ligand, which is as yet not identified in $AhR^{+/+}$ mice. In response to such an AhR-null effect, $AhR^{-/-}$ mice reversely show extensive hematopoiesis in the spleen (Fig. 8(b)) as compared with wild-type mice (Fig. 8(a)), although this hemopoietic enhancement is also reflected in another negative hemopoietic regulation in the bone marrow.

3.2.3. AhR promotes cell cycling in hemopoietic progenitors

Interestingly, when bone marrow cells are removed from $AhR^{-/-}$ mice and $AhR^{+/+}$ mice, and are grown in *in vitro* colony assay, the numbers of CFU-GM and CFU-E are both significantly lower in $AhR^{-/-}$ mice (Fig. 7(c)), implying that AhR signaling promotes the acute phase response to cytokines during colony growth. The decrease in the number of CFU-E, as shown in Fig. 7(c), possibly affects the number of RBCs in the peripheral blood of $AhR^{-/-}$ mice (Fig. 7(a)). These observations are consistent with those for other hemopoietic progenitors (data not shown). Interestingly, in response to such an AhR-null effect, AhR-KO mice in contrast show extensive hemopoiesis in the spleen (Fig. 7(d)), which results in a significant increase in spleen weight (Fig. 7(a); rightmost) [28,91].

3.3. *Cell kinetics of CFU-GM receives negative feedback in steady state*

The BUUV method[1] shows a clear enhancement of the cell cycle in primitive progenitor cells, CFU-S-13 (Fig. 9(a)), and in

[1] BUUV method is to evaluate hematopoietic stem/progenitor cell-specific kinetics by continuous perfusion of 5-bromo-2′-deoxyuridine (BrdUrd) through an osmotic pump (Alza Corp., Palo Alto, CA) followed by ultraviolet (UV) – A exposure and hematopoietic colonization assay, which permits to obtain a variety of parameters in the cell kinetics of the hemopoietic progenitor cell compartment, such as a doubling time, a size of cycling- or quiescent fraction, and also the size of cycling fraction during the unit time interval.

relatively mature progenitor cells, CFU-S-9 (Fig. 9(b)) in $AhR^{-/-}$ mice. Although the precise mechanism underlying this phenomenon is not clarified yet, the cell kinetics of CFU-GM becomes suppressed in terms of percent cycling fraction per unit time, i.e., less than 5% (Fig. 9(c)), which may be due to a possible negative feedback to an up-regulated cell kinetics of primitive progenitors (Fig. 9(a) and (b)).

The lack of AhR and the complex compensation of bone marrow hematopoiesis might still be insufficient in $AhR^{+/+}$ mice, because a compensatory increase in splenic weight in $AhR^{-/-}$ mice is evident (Figs. 7(a) and 8). As reported by Puga et al. [86], AhR functions as a cell-cycle regulator rather than as a drug-metabolizing enzyme inducer; thus, possible phenotypes transmitted via AhR may be diversified.

4. Hematopoietic progenitor cells and xenobiotic responses

By analyzing antioxidative responses to thioredoxin concerns, we have recently found that benzene-induced xenobiotic responses are associated with antioxidative signaling [92]. Thus, the increased incidence of spontaneous neoplasms and accelerated aging observed in AhR-KO mice can be hypothesized as consequences of genomic instability possibly due to the absence of xenobiotic or antioxidative responses. ROSs in hematopoietic tissues in both AhR-KO and wild-type mice were evaluated using the DCFH-DA dye by flow cytometry, followed by the fractionation of hematopoietic progenitor cells. Hematopoietic tissues from $AhR^{-/-}$ mice showed a high reactivity to DCFH-DA, as shown in Fig. 5. Because the AhR expression level is high on primitive hematopoietic progenitor cells [91] fractionated primitive hematopoietic progenitor cells were also evaluated for their reactivity to DCFH-DA, which was found to be higher than the reactivity of other unfractionated bone marrow cells. Hematopoietic progenitor cells, i.e., the LKS fraction, are quiescent in an anoxic environment; furthermore, its activity is regulated by weak oxidative tension. Thus, the higher reactivity of the hematopoietic progenitor cell fraction in $AhR^{-/-}$ mice to the DCFH-DA dye is considered to be in good agreement with the underlying mechanism of genomic stability of wild-type $AhR^{+/+}$ mice, which may be linked to the suppressive function of AhR and the consequent longevity.

4.1. *Aryl-hydrocarbon-receptor-mediated hematopoietic alteration by xenobiotic substances*

When xenobiotic ligands such as TCDD and/or benzo[*a*]pyrene are applied to AhRs, transcription of drug-metabolizing enzymes such as Cyp1A1 and 1B1 are induced [1,2]. The consequent induction of oxidative stress by these induced Cyp1A1 and 1B1 is known precisely [6,77]. The function of AhR in relation to the hematopoietic system involves two possible factors for hematopoiesis. First, induction of Cyp1A1 and 1B1 by xenobiotic responses consequently induces up-regulation of a cyclin-dependent kinase inhibitor, $p27^{kip1}$ or $p21^{waf1}$, which readily suppresses the cell cycle [78,79]. Benzene is a unique newly found chemical whose toxicity is mediated by AhR [69], which suppresses the hematopoietic stem-cell-specific cell cycle [93], which will be introduced as a model of hematopoietic stem cell modulation in the next section.

Second, what happens in the primitive hematopoietic stem cell system when AhR is stimulated by ligand-dependent up-regulation? In this situation, ARNT required by Hif-1alpha and Hif-2alpha in the hypoxic hematopoietic microenvironment is considered to inhibit primitive hematopoiesis [78]. Because of this suppression of primitive hematopoiesis, various hematopoietic progenitor cell compartments are decreased in number, as observed by Luster et al. in a variety of CFUs after exposure of mice to TCDD [76,88].

The above-mentioned hematopoietic impairment is based on the impaired function of the long-term reconstitution activity of the LKS fraction, i.e., primitive hematopoietic progenitor compartment. The long-term reconstitution activity of the LKS fraction repopulated in lethal-dose-irradiated recipients was heavily impaired after TCDD exposure. When repopulation of the LKS fraction is applied following TCDD exposure, while the nontreated LKS fraction successfully reaches a chimeric ratio of 80% with respect to the competitive donor fraction by 140 days after transplantation, the chimeric ratio is limited only to 15% with peak at 80 days after transplantation and the LKS fraction exposed to TCDD disappears by 140 days after transplantation [94].

Similar lymphopoietic alterations are observed after exposure to TCDD such as inhibition of thymic cell development [95], dysregulation of regulatory T and pro-inflammatory T cell differentiation [96], alteration of B cell maturation and CD34-positive human hematopoietic progenitor cells [97]. These alterations are also observed for ligands other than TCDD [96,98].

4.2. *Aryl-hydrocarbon-receptor-mediated benzene hematotoxicities*

Recent studies have shown that AhR in primitive cells transmits negative signals for the proliferation of such cells [91]. As we previously reported, primitive hemopoietic progenitor cells increases in number in AhR-KO mice; on the other hand, relatively mature progenitor cells, decreases in number in a homeostatic manner [91].

We have reported that benzene-induced hemopoietic toxicity is transmitted by AhR [69]. We also found that CYP2E1 related to benzene metabolism is also up-regulated in the bone marrow following benzene exposure [99]. Therefore, it is of interest to hypothesize a greater role of bone marrow cells in hemopoietic toxicity than in hepatic metabolism. Accordingly, in our present study, benzene-induced hemopoietic toxicity was evaluated in wild-type mice after a lethal dose of whole-body irradiation followed by repopulation with bone marrow cells that lack AhR or, *vice versa*, in AhR-KO mice after repopulation with wild-type bone marrow cells. As a result, benzene-induced hemopoietic toxicity seems to have been transmitted through AhR, and benzene was transformed by *de novo* metabolism with CYP2E1 in the bone marrow.

Six weeks after the repopulation, the steady-state hematopoietic parameters for repopulated mice were obtained and are shown in Fig. 10. The results were essentially the same between the mice repopulated with wild-type bone marrow

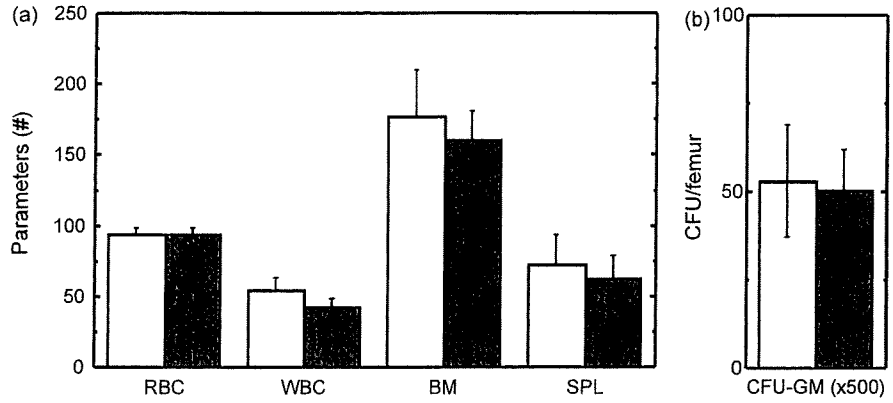

Fig. 10 – Comparison of various blood parameters between mice repopulated with wild-type BM (open columns) and AhR-KO ($AhR^{-/-}$) BM (shaded columns) cells; (a) peripheral blood, BM and spleen weight. #: Vertical axis "Parameters" indicates the counts of peripheral RBCs ($\times 10^8$/ml) and WBCs ($\times 10^6$/ml), BM cellularity ($\times 10^5$/femur), and weight of spleen (SPL, mg). (b) Numbers of CFU-GM (5×10^2/femur) per femur.

cells (open columns) and those repopulated with AhR-KO bone marrow cells (shaded columns).

Fig. 11(a) and (b) show the percentages of RBCs (a) and WBCs (b) with respect to that of the control in the peripheral blood after the repopulation with bone marrow cells. In the wild-type mice repopulated with wild-type bone marrow cells and those with AhR-KO bone marrow cells (open and closed symbols, respectively), benzene exposure induced a slight but statistically significant decrease in RBC count compared with the sham exposure except on day 5 in the wild-type group (100% with standard deviation of the mean indicated by horizontal lines: Fig. 11(a)). The dose used in our present study was sufficiently high, and the decrease in RBC count was readily observed within two weeks of exposure.

The decreases in WBC count shown in Fig. 11(b) are more significant than those in RBC count throughout the exposure period except on day 5 in the AhR-KO group (the data were significantly different between wild-type mice (50.8 ± 11.2%) and AhR-KO mice (70.6 ± 17.6%; $p = 0.024$)).

As shown in Fig. 11(c), the decrease in the number of bone marrow cells after benzene exposure is significant in the mice repopulated with wild-type bone marrow cells specifically on

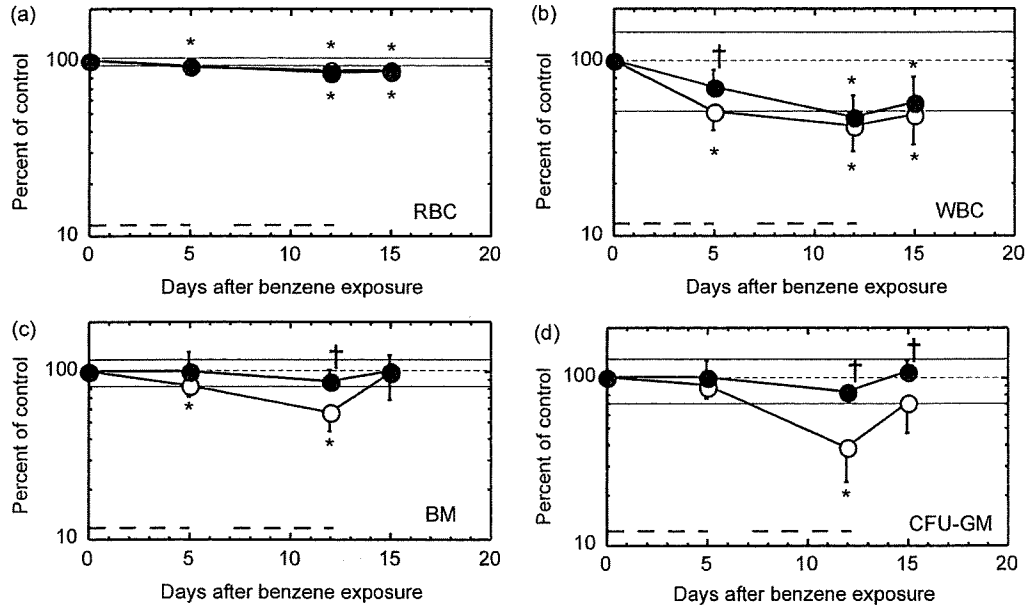

Fig. 11 – Changes in percentage of RBCs (a), WBCs (b), BM cells (c) and CFU-GM (d) of mice repopulated with wild-type BM (open symbols) and AhR-KO ($AhR^{-/-}$) BM (closed symbols) cells during and after benzene exposure, with respect to those in each sham-exposure group. Vertical bars indicate the standard deviation of the mean. Horizontal dashed line indicates the mean (100%) and the solid lines indicate the standard deviation of the mean (100%) from the sham-exposure control wild-type group. The dashed line at the bottom indicates benzene exposure duration.
***: Significant difference between sham-exposure group and benzene-exposed group determined by t-test at $p < 0.05$.**
†: Significant difference between wild-type mice and AhR-KO mice.

days 5 and 12 (82.2 ± 12.0%, $p = 0.035$ and 65.4 ± 20.3%, $p = 0.007$, respectively; number of cells obtained on day 12, significantly different between the wild-type mice and the AhR-KO mice (75.4 ± 19.7%; $p = 0.014$)), which returned to the normal range by day 15, that is, 3 days after cessation of benzene treatment. In contrast to the peripheral blood parameters (Fig. 11(a) and (b)), the number of bone marrow cells in the mice repopulated with AhR-KO bone marrow cells did not show any decrease, but the mice showed a clear nullification of benzene-induced decrease in the number of bone marrow cells (86.7 ± 14.9%; $p = 0.057$). Concerning the weight of the spleen, there are no significant differences among the groups regardless of the duration of benzene treatment and AhR expression level (not shown).

In Fig. 11(d), the number of CFU-GM in the bone marrow of mice repopulated with wild-type bone marrow cells much more significantly decreased on day 12 (open symbols, 37.8 ± 14.2%, $p = 0.019$; number of cells, significantly different between wild-type mice and AhR-KO mice (82.0 ± 7.0%; $p = 0.001$)), which rapidly returned to the normal range by day 15, 3 days after cessation of benzene treatment. As shown in this figure, interestingly, the benzene-induced decrease in the number of CFU-GM in the bone marrow of mice repopulated with the AhR-KO bone marrow cells (closed symbols) is clearly nullified for the wild-type bone marrow cells (open symbols), and the number remains within the range found for the sham exposure. The reason for this very prominent decrease in the number of CFU-GM observed in the case of benzene exposure may be due, in part, to the expression of AhR, whose level is significantly high in primitive hematopoietic progenitor cells [5,100]. The KO of AhR nullified the decrease in the number of CFU-GM much more significantly than the decrease in peripheral blood parameters.

5. Summary

Oxidative stress induced by AhR-mediated benzene metabolites induces xenobiotic hematological malignancies in C57BL/6 mice. The encounter of AhR with benzene may not be the original biological relevance of historic and phylogenic evolution of the AhR molecule in a wide range of animals from invertebrates to vertebrates including humans. Would not this be an ironical encounter?

In experimental mice, the existence of AhR apparently extends their lifespan as compared with AhR-KO mice (mean life spans, 756 days in AhR-homozygous KO and 890 days in wild-type C57BL/6). The major reasons for this extension of lifespan by AhRs seem to be the suppression of epigenetic tumorigenicity and age-related gerontological diseases, possibly owing to the advantages derived in reducing oxidative stresses through the AhR function. No precise mechanism has been reported, but the onset of spontaneous neoplasms and non-neoplastic senescent diseases is delayed in wild-type mice as compared with that in AhR-deficient mice. Furthermore, when *AhR* is knocked out, in the case of the hematopoietic system, the capacity to maintain the hematopoietic stem cell compartment is clearly diminished and the major fraction tends to differentiate into descendant blood cell classes. The hematopoietic stem cell compartment shows the following. First, the compartment shows a diminished capacity to maintain the LKS fraction, the stem cell compartment, as observed by cell sorting analysis. Second, it shows a decrease in the fraction of the dormant stem cell/progenitor compartment, as measured by the BUUV method for evaluating kinetics of hematopoietic progenitor cells, by continuous in vivo treatment with BrdUrd and BrdUrd-labeled cell-purging with ultraviolet (UV) light. Thus, the possible regulation of hematopoietic stem cells maintaining the fraction of dormant hematopoietic stem cells may have mechanistic relevance in terms of a possible genomic stabilization by AhR, which should be elucidated.

The hematopoietic microenvironment is hypoxic during the steady state. This hypoxic state induces AhR to release (unbound) ARNT to Hif-1alpha as well as Hif-2alpha; thus, the function of slight changes in regulating oxidative stress for a hematopoietic trigger in the hematopoietic microenvironment in wild-type mice may not be markedly different from that in the AhR-KO mice. However, when a change induces a much higher extent of oxidative stress induced by substances such as hydrogen peroxide in AhR-KO mice, the increased amount of ROSs is readily detected in AhR-KO mice, whereas wild-type mice show active removal of oxidative stress by ROS-scavenging molecules, resulting in notable differences in the amount of ROSs between wild-type and AhR-KO mice (Fig. 5).

Evidence was found in the liver that the expression of antioxidative stress genes such as superoxide dismutase 1 (Cu/Zn-SOD) and SOD2 (Mn-SOD) genes, as well as the Trx gene, which is located downstream of AhR and carrying XRE, are more highly expressed in wild-type mice than in AhR-KO mice [63].

In contrast to the above-mentioned beneficial biological function of AhR, in the case of benzene exposure, benzene exposure induces hematopoietic disturbances and the consequent leukemias. This seems to be induced by oxidative stress in AhR wild-type mice because Trx-overexpressing mice in contrast show nullification of hematopoietic disturbances owing to oxidative stress removal. Here is an enigma of benzene-induced hematotoxicity, that is, oxidative stress induced by as low as one part per million of benzene, which cannot be removed by antioxidative molecules associated with AhR as compared with those induced by hydrogen peroxide. On the other hand, the benzene exposure of AhR-KO mice is supposed to show none of the benzene-mediated oxidative-stress-induced hematopoietic disturbances or myeloid leukemias, simply owing to nullification of benzene metabolism in these mice lacking AhR.

Acknowledgments

We thank Ms. E. Tachihara, Ms. Y. Kondo, Ms. C. Aoyagi, Ms. Y. Usami, Ms. Y. Shinzawa, and Ms. M. Uchiyama for excellent technical assistance, and Ms. N. Kikuchi, M. Yoshizawa, and Ms. M. Hojo for secretarial assistance. Encouragement of the study and the review of the manuscript by Prof. Fumio Matsumura is also appreciated.

This work was supported in part by a Grant-in-Aid for Scientific Research C, 15510064, 18510066 and also by the

MHLW-Research Fund (H19-Chemistry 003), National Institute of Health Sciences.

REFERENCES

[1] de Oliveira SK, Hoffmeister M, Gambaryan S, Muller-Esterl W, Guimaraes JA, Smolenski AP. Phosphodiesterase 2A forms a complex with the co-chaperone XAP2 and regulates nuclear translocation of the aryl hydrocarbon receptor. J Biol Chem 2007;282:13656–63.

[2] Gu YZ, Hogenesch JB, Bradfield CA. The PAS superfamily: sensors of environmental and developmental signals. Annu Rev Pharmacol Toxicol 2000;40:519–61.

[3] Duan R, Porter W, Samudio I, Vyhlidal C, Kladde M, Safe S. Transcriptional activation of c-fos protooncogene by 17beta-estradiol: mechanism of aryl hydrocarbon receptor-mediated inhibition. Mol Endocrinol 1999;13:1511–21.

[4] Hahn ME. Aryl hydrocarbon receptors: diversity and evolution. Chem Biol Interact 2002;141:131–60.

[5] Hirabayashi Y, Miyajima A, Yokota T, Arai K, Li G, Yoon B, et al. Effect of 2,3,7,8-tetrachlorodibenzo-p-dioxin (TCDD) on B cell differentiation in mouse pre-B colonization model regulated by artificially introduced human IL-3 receptors. Organohalogen Compd 2002;53:332–5.

[6] Dalton TP, Puga A, Shertzer HG. Induction of cellular oxidative stress by aryl hydrocarbon receptor activation. Chem Biol Interact 2002;141:77–95.

[7] Trosko JE, Inoue T. Oxidative stress, signal transduction, and intercellular communication in radiation carcinogenesis. Stem Cells 1997;15(Suppl. 2):59–67.

[8] Gershon-Cohen J, Hermel MB, Griffith Jr JQ. The value of small lead shields against the injurious effect of total-body irradiation. Science 1951;114:157–8.

[9] Till JE, McCulloch EA. A direct measurement of the radiation sensitivity of normal mouse bone marrow cells. Radiat Res 1961;14:213–22.

[10] Lewis JP, Trobaugh Jr FE. Haematopoietic stem cells. Nature 1964;204:589–90.

[11] Pluznik DH, Sachs L. The cloning of normal "mast" cells in tissue culture. J Cell Physiol 1965;66:319–24.

[12] Bradley TR, Metcalf D. The growth of mouse bone marrow cells in vitro. Aust J Exp Biol Med Sci 1966;44:287–99.

[13] Harrison DE. Mouse erythropoietic stem cell lines function normally 100 months: loss related to number of transplantations. Mech Ageing Dev 1979;9:427–33.

[14] Cronkite EP. Regulation and structure of heemopoiesis: its application in toxicology. In: Irons RD, editor. Toxicology of the blood and bone marrow. New York: Raven Press; 1985.

[15] Rosendaal M, Hodgson GS, Bradley TR. Organization of haemopoietic stem cells: the generation-age hypothesis. Cell Tissue Kinet 1979;12:17–29.

[16] Okada S, Nakauchi H, Nagayoshi K, Nishikawa S, Miura Y, Suda T. In vivo and in vitro stem cell function of c-kit- and Sca-1-positive murine hematopoietic cells. Blood 1992;80:3044–50.

[17] Hirabayashi Y, Yoon BI, Tsuboi I, Huo Y, Kodama Y, Kanno J, et al. Membrane channel connexin 32 maintains Lin(−)/c-kit (+) hematopoietic progenitor cell compartment: analysis of the cell cycle. J Membr Biol 2007;217:105–13.

[18] Rudolph KL, Chang S, Lee HW, Blasco M, Gottlieb GJ, Greider C, et al. Longevity, stress response, and cancer in aging telomerase-deficient mice. Cell 1999;96:701–12.

[19] Zhang J, Niu C, Ye L, Huang H, He X, Tong WG, et al. Identification of the haematopoietic stem cell niche and control of the niche size. Nature 2003;425:836–41.

[20] Puch S, Armeanu S, Kibler C, Johnson KR, Muller CA, Wheelock MJ, et al. N-cadherin is developmentally regulated and functionally involved in early hematopoietic cell differentiation. J Cell Sci 2001;114:1567–77.

[21] Calvi LM, Adams GB, Weibrecht KW, Weber JM, Olson DP, Knight MC, et al. Osteoblastic cells regulate the haematopoietic stem cell niche. Nature 2003;425:841–6.

[22] Mancini SJ, Mantei N, Dumortier A, Suter U, MacDonald HR, Radtke F. Jagged1-dependent Notch signaling is dispensable for hematopoietic stem cell self-renewal and differentiation. Blood 2005;105:2340–2.

[23] Arai F, Hirao A, Ohmura M, Sato H, Matsuoka S, Takubo K, et al. Tie2/angiopoietin-1 signaling regulates hematopoietic stem cell quiescence in the bone marrow niche. Cell 2004;118:149–61.

[24] Nilsson SK, Johnston HM, Whitty GA, Williams B, Webb RJ, Denhardt DT, et al. Osteopontin, a key component of the hematopoietic stem cell niche and regulator of primitive hematopoietic progenitor cells. Blood 2005;106:1232–9.

[25] Nagasawa T, Hirota S, Tachibana K, Takakura N, Nishikawa S, Kitamura Y, et al. Defects of B-cell lymphopoiesis and bone-marrow myelopoiesis in mice lacking the CXC chemokine PBSF/SDF-1. Nature 1996;382:635–8.

[26] Zou YR, Kottmann AH, Kuroda M, Taniuchi I, Littman DR. Function of the chemokine receptor CXCR4 in haematopoiesis and in cerebellar development. Nature 1998;393:595–9.

[27] Hirabayashi Y, Yoon BI, Tsuboi I, Huo Y, Kodama Y, Kanno J, et al. Protective role of connexin 32 in steady-state hematopoiesis, regeneration state, and leukemogenesis. Exp Biol Med (Maywood) 2007;232:700–12.

[28] Hirabayashi Y, Yoon BI, Li GX, Fujii-Kuriyama Y, Kaneko T, Kanno J, et al. Benzene-induced hematopoietic toxicity transmitted by AhR in the wild-type mouse was negated by repopulation of AhR deficient bone marrow cells. Organohalogen Compd 2005;67:2280–3.

[29] Yoshida K, Aizawa S, Watanabe K, Hirabayashi Y, Inoue T. Stem-cell leukemia: p53 deficiency mediated suppression of leukemic differentiation in C3H/He myeloid leukemia. Leuk Res 2002;26:1085–92.

[30] Yoshida K, Hirabayashi Y, Wada S, Watanabe F, Watanabe K, Aizawa S, et al. p53 (TRP53) deficiency-mediated antiapoptosis escape after 5 Gy X irradiation still induces stem cell leukemia in C3H/He mice: comparison between whole-body assay and bone marrow transplantation (BMT) assay. Radiat Res 2007;167:703–10.

[31] Kondo M, Weissman IL, Akashi K. Identification of clonogenic common lymphoid progenitors in mouse bone marrow. Cell 1997;91:661–72.

[32] Wolf NS, Trentin JJ. Hemopoietic colony studies. V. Effect of hemopoietic organ stroma on differentiation of pluripotent stem cells. J Exp Med 1968;127:205–14.

[33] Ploemacher RE, Mayen AE, De Koning AE, Krenacs T, Rosendaal M. Hematopoiesis: gap junction intercellular communication is likely to be involved in regulation of stroma-dependent proliferation of hemopoietic stem cells. Hematology 2000;5:133–47.

[34] Minami A, Tsuboi I, Harada T, Fukumoto T, Hiramoto M, Koshinaga M, et al. Inflammatory biomarker, neopterin, suppresses B lymphopoiesis for possible facilitation of granulocyte responses, which is severely altered in age-related stromal-cell-impaired mice, SCI/SAM. Exp Biol Med (Maywood) 2007;232:134–45.

[35] Hahn ME. The aryl hydrocarbon receptor: a comparative perspective. Comp Biochem Physiol C Pharmacol Toxicol Endocrinol 1998;121:23–53.

[36] Ema M, Sogawa K, Watanabe N, Chujoh Y, Matsushita N, Gotoh O, et al. cDNA cloning and structure of mouse putative Ah receptor. Biochem Biophys Res Commun 1992;184:246–53.
[37] Burbach KM, Poland A, Bradfield CA. Cloning of the Ah-receptor cDNA reveals a distinctive ligand-activated transcription factor. Proc Natl Acad Sci USA 1992;89:8185–9.
[38] Schmidt JV, Carver LA, Bradfield CA. Molecular characterization of the murine Ahr gene. Organization, promoter analysis, and chromosomal assignment. J Biol Chem 1993;268:22203–9.
[39] Dolwick KM, Schmidt JV, Carver LA, Swanson HI, Bradfield CA. Cloning and expression of a human Ah receptor cDNA. Mol Pharmacol 1993;44:911–7.
[40] Poland A, Palen D, Glover E. Analysis of the four alleles of the murine aryl hydrocarbon receptor. Mol Pharmacol 1994;46:915–21.
[41] Chang C, Smith DR, Prasad VS, Sidman CL, Nebert DW, Puga A. Ten nucleotide differences, five of which cause amino acid changes, are associated with the Ah receptor locus polymorphism of C57BL/6 and DBA/2 mice. Pharmacogenetics 1993;3:312–21.
[42] Carver LA, Hogenesch JB, Bradfield CA. Tissue specific expression of the rat Ah-receptor and ARNT mRNAs. Nucleic Acids Res 1994;22:3038–44.
[43] Pohjanvirta R, Wong JM, Li W, Harper PA, Tuomisto J, Okey AB. Point mutation in intron sequence causes altered carboxyl-terminal structure in the aryl hydrocarbon receptor of the most 2,3,7,8-tetrachlorodibenzo-p-dioxin-resistant rat strain. Mol Pharmacol 1998;54:86–93.
[44] Korkalainen M, Tuomisto J, Pohjanvirta R. Restructured transactivation domain in hamster AH receptor. Biochem Biophys Res Commun 2000;273:272–81.
[45] Kim EY, Hahn ME, Iwata H, Tanabe S, Miyazaki N. cDNA cloning of an aryl hydrocarbon receptor from Baikal seals (Phoca sibirica). Mar Environ Res 2002;54:285–9.
[46] Walker MK, Heid SE, Smith SM, Swanson HI. Molecular characterization and developmental expression of the aryl hydrocarbon receptor from the chick embryo. Comp Biochem Physiol C Toxicol Pharmacol 2000;126:305–19.
[47] Karchner SI, Kennedy SW, Trudeau S, Hahn ME. Towards molecular understanding of species differences in dioxin sensitivity: initial characterization of Ah receptor cDNAs in birds and an amphibian. Mar Environ Res 2000;50:51–6.
[48] Karchner SI, Powell WH, Hahn ME. Identification and functional characterization of two highly divergent aryl hydrocarbon receptors (AHR1 and AHR2) in the teleost Fundulus heteroclitus. Evidence for a novel subfamily of ligand-binding basic helix loop helix-Per-ARNT-Sim (bHLH-PAS) factors. J Biol Chem 1999;274:33814–2.
[49] Tanguay RL, Abnet CC, Heideman W, Peterson RE. Cloning and characterization of the zebrafish (Danio rerio) aryl hydrocarbon receptor. Biochim Biophys Acta 1999;1444:35–48.
[50] Besselink HT, Denison MS, Hahn ME, Karchner SI, Vethaak AD, Koeman JH, et al. Low inducibility of CYP1A activity by polychlorinated biphenyls (PCBs) in flounder (Platichthys flesus): characterization of the Ah receptor and the role of CYP1A inhibition. Toxicol Sci 1998;43:161–71.
[51] Abnet CC, Tanguay RL, Hahn ME, Heideman W, Peterson RE. Two forms of aryl hydrocarbon receptor type 2 in rainbow trout (Oncorhynchus mykiss). Evidence for differential expression and enhancer specificity. J Biol Chem 1999;274:15159–66.
[52] Karchner SI, Franks DG, Powell WH, Hahn ME. Regulatory interactions among three members of the vertebrate aryl hydrocarbon receptor family: AHR repressor, AHR1, and AHR2. J Biol Chem 2002;277:6949–59.
[53] Hahn ME, Karchner SI, Shapiro MA, Perera SA. Molecular evolution of two vertebrate aryl hydrocarbon (dioxin) receptors (AHR1 and AHR2) and the PAS family. Proc Natl Acad Sci USA 1997;94:13743–8.
[54] Butler RA, Kelley ML, Powell WH, Hahn ME, Van Beneden RJ. An aryl hydrocarbon receptor (AHR) homologue from the soft-shell clam, Mya arenaria: evidence that invertebrate AHR homologues lack 2,3,7,8-tetrachlorodibenzo-p-dioxin and beta-naphthoflavone binding. Gene 2001;278:223–34.
[55] Duncan DM, Burgess EA, Duncan I. Control of distal antennal identity and tarsal development in Drosophila by spineless-aristapedia, a homolog of the mammalian dioxin receptor. Genes Dev 1998;12:1290–303.
[56] Emmons RB, Duncan D, Estes PA, Kiefel P, Mosher JT, Sonnenfeld M, et al. The spineless-aristapedia and tango bHLH-PAS proteins interact to control antennal and tarsal development in Drosophila. Development 1999;126:3937–45.
[57] Wernet MF, Mazzoni EO, Celik A, Duncan DM, Duncan I, Desplan C. Stochastic spineless expression creates the retinal mosaic for colour vision. Nature 2006;440:174–80.
[58] Huang X, Powell-Coffman JA, Jin Y. The AHR-1 aryl hydrocarbon receptor and its co-factor the AHA-1 aryl hydrocarbon receptor nuclear translocator specify GABAergic neuron cell fate in *C. elegans*. Development 2004;131:819–28.
[59] Qin H, Powell-Coffman JA. The *Caenorhabditis elegans* aryl hydrocarbon receptor, AHR-1, regulates neuronal development. Dev Biol 2004;270:64–75.
[60] Nebert DW, Brown DD, Towne DW, Eisen HJ. Association of fertility, fitness and longevity with the murine Ah locus among (C57BL/6N) (C3H/HeN) recombinant inbred lines. Biol Reprod 1984;30:363–73.
[61] Gompertz B. On the nature of the function expressive of the law of human mortality, and on a new mode of determining the value of life contingencies. Pholos Trans Royal Soc (London) 1825;115:513–85.
[62] Hirabayashi Y, Yoon BI, Li GX, Fujii-Kuriyama Y, Kaneko T, Kanno J, et al. Tumor suppressor function of aryl hydrocarbon receptor (AhR): early onsets of spontaneous lymphoma and hepatoma, and resulting shortened life span observed in AhR deficient mice. Organohalogen Compd 2006;68:556–9.
[63] Hirabayashi Y, Yoon BI, Li GX, Kanno J, Fujii-Kuriyama Y, Inoue T. Aryl hydrocarbon receptor suppresses spontaneous neoplasms and extends life span: possible mechanism implied by hematopoietic stem cell kinetics. Organohalogen Compd 2007;69:357–61.
[64] Zou GM, Luo MH, Reed A, Kelley MR, Yoder MC. Ape1 regulates hematopoietic differentiation of embryonic stem cells through its redox functional domain. Blood 2007;109:1917–22.
[65] Sakuma T, Ohtake M, Katsurayama Y, Jarukamjorn K, Nemoto N. Induction of CYP1A2 by phenobarbital in the livers of aryl hydrocarbon-responsive and -nonresponsive mice. Drug Metab Dispos 1999;27:379–84.
[66] Poland A, Glover E, Taylor BA. The murine Ah locus: a new allele and mapping to chromosome 12. Mol Pharmacol 1987;32:471–8.
[67] Van Zant G, de Haan G. Genetic control of lifespan: studies from animal models. Expert Rev Mol Med 1999;1999:1–12.
[68] Forster MJ, Morris P, Sohal RS. Genotype and age influence the effect of caloric intake on mortality in mice. FASEB J 2003;17:690–2.
[69] Yoon BI, Hirabayashi Y, Kawasaki Y, Kodama Y, Kaneko T, Kanno J, et al. Aryl hydrocarbon receptor mediates benzene-induced hematotoxicity. Toxicol Sci 2002;70:150–6.

[70] Abbott BD, Birnbaum LS, Perdew GH. Developmental expression of two members of a new class of transcription factors: I. Expression of aryl hydrocarbon receptor in the C57BL/6N mouse embryo. Dev Dyn 1995;204:133–43.
[71] Spindler SR, Koizumi A, Walford RL, Mote PL. P1-450 and P3-450 gene expression and maximum life span in mice. Mutat Res 1989;219:89–94.
[72] Inoue T, Hirabayashi Y, Mitsui H, Sasaki H, Cronkite EP, Bullis Jr JE, et al. Survival of spleen colony-forming units (CFU-S) of irradiated bone marrow cells in mice: evidence for the existence of a radioresistant subfraction. Exp Hematol 1995;23:1296–300.
[73] Ceradini DJ, Kulkarni AR, Callaghan MJ, Tepper OM, Bastidas N, Kleinman ME, et al. Progenitor cell trafficking is regulated by hypoxic gradients through HIF-1 induction of SDF-1. Nat Med 2004;10:858–64.
[74] Levesque JP, Winkler IG, Hendy J, Williams B, Helwani F, Barbier V, et al. Hematopoietic progenitor cell mobilization results in hypoxia with increased hypoxia-inducible transcription factor-1 alpha and vascular endothelial growth factor A in bone marrow. Stem Cells 2007;25:1954–65.
[75] Tian H, McKnight SL, Russell DW. Endothelial PAS domain protein 1 (EPAS1), a transcription factor selectively expressed in endothelial cells. Genes Dev 1997;11:72–82.
[76] Luster MI, Hong LH, Boorman GA, Clark G, Hayes HT, Greenlee WF, et al. Acute myelotoxic responses in mice exposed to 2,3,7,8-tetrachlorodibenzo-p-dioxin (TCDD). Toxicol Appl Pharmacol 1985;81:156–65.
[77] Chen ZH, Hurh YJ, Na HK, Kim JH, Chun YJ, Kim DH, et al. Resveratrol inhibits TCDD-induced expression of CYP1A1 and CYP1B1 and catechol estrogen-mediated oxidative DNA damage in cultured human mammary epithelial cells. Carcinogenesis 2004;25:2005–13.
[78] Wang G, Reisdorph R, Clark Jr RE, Miskimins R, Lindahl R, Miskimins WK. Cyclin dependent kinase inhibitor p27(Kip1) is upregulated by hypoxia via an ARNT dependent pathway. J Cell Biochem 2003;90: 548–60.
[79] Pang PH, Lin YH, Lee YH, Hou HH, Hsu SP, Juan SH. Molecular mechanisms of p21 and p27 induction by 3-methylcholanthrene, an aryl-hydrocarbon receptor agonist, involved in antiproliferation of human umbilical vascular endothelial cells. J Cell Physiol 2008;215:161–71.
[80] Hirabayashi Y, Matsumura T, Matsuda M, Kuramoto K, Motoyoshi K, Yoshida K, et al. Cell kinetics of hemopoietic colony-forming units in spleen (CFU-S) in young and old mice. Mech Ageing Dev 1998;101:221–31.
[81] Staller P, Sulitkova J, Lisztwan J, Moch H, Oakeley EJ, Krek W. Chemokine receptor CXCR4 downregulated by von Hippel-Lindau tumour suppressor pVHL. Nature 2003;425:307–11.
[82] Ramirez-Bergeron DL, Runge A, Adelman DM, Gohil M, Simon MC. HIF-dependent hematopoietic factors regulate the development of the embryonic vasculature. Dev Cell 2006;11:81–92.
[83] Le Bras A, Lionneton F, Mattot V, Lelievre E, Caetano B, Spruyt N, et al. HIF-2alpha specifically activates the VE-cadherin promoter independently of hypoxia and in synergy with Ets-1 through two essential ETS-binding sites. Oncogene 2007;26:7480–9.
[84] Adelman DM, Maltepe E, Simon MC. Multilineage embryonic hematopoiesis requires hypoxic ARNT activity. Genes Dev 1999;13:2478–83.
[85] Adachi J, Mori Y, Matsui S, Takigami H, Fujino J, Kitagawa H, et al. Indirubin and indigo are potent aryl hydrocarbon receptor ligands present in human urine. J Biol Chem 2001;276:31475–8.
[86] Puga A, Xia Y, Elferink C. Role of the aryl hydrocarbon receptor in cell cycle regulation. Chem Biol Interact 2002;141:117–30.
[87] Mimura J, Yamashita K, Nakamura K, Morita M, Takagi TN, Nakao K, et al. Loss of teratogenic response to 2,3,7.8-tetrachlorodibenzo-p-dioxin (TCDD) in mice lacking the Ah (dioxin) receptor. Genes Cells 1997;2:645–54.
[88] Luster MI, Boorman GA, Dean JH, Harris MW, Luebke RW, Padarathsingh ML, et al. Examination of bone marrow, immunologic parameters and host susceptibility following pre- and postnatal exposure to 2,3,7,8-tetrachlorodibenzo-p-dioxin (TCDD). Int J Immunopharmacol 1980;2:301–10.
[89] Yoon BI, Hirabayashi Y, Kaneko T, Kodama Y, Kanno J, Yodoi J, et al. Transgene expression of thioredoxin (trx/adf) protects against 2,3,7,8-tetrachlorodibenzo-p-dioxin (tcdd)-induced hematotoxicity. Arch Environ Contam Toxicol 2001;41:232–6.
[90] Yoon BI, Hirabayashi Y, Kaneko T, Kodama Y, Kanno J, Yodoi J, et al. Transgene expression of thioredoxin (TRX/ADF) protects against 2,3,7,8-tetrachlorodibenzo-P-dioxin (TCDD)-induced hematotoxicity. Organohalogen Compd 2001;53:332–5.
[91] Hirabayashi Y, Li GX, Yoon BI, Fujii-Kuriyama Y, Kaneko T, Kanno J, et al. AhR suppresses hemopoiesis during steady state but accelerates cell cycle as an early response: a study of AhR-knockout mice. Organohalogen Compd 2003;64:270–3.
[92] Li GX, Hirabayashi Y, Yoon BI, Kawasaki Y, Tsuboi I, Kodama Y, et al. Thioredoxin overexpression in mice, model of attenuation of oxidative stress, prevents benzene-induced hemato-lymphoid toxicity and thymic lymphoma. Exp Hematol 2006;34:1687–97.
[93] Yoon BI, Hirabayashi Y, Kawasaki Y, Kodama Y, Kaneko T, Kim DY, et al. Mechanism of action of benzene toxicity: cell cycle suppression in hemopoietic progenitor cells (CFU-GM). Exp Hematol 2001;29:278–85.
[94] Sakai R, Kajiume T, Inoue H, Kanno R, Miyazaki M, Ninomiya Y, et al. TCDD treatment eliminates the long-term reconstitution activity of hematopoietic stem cells. Toxicol Sci 2003;72:84–91.
[95] Svensson C, Silverstone AE, Lai ZW, Lundberg K. Dioxin-induced adseverin expression in the mouse thymus is strictly regulated and dependent on the aryl hydrocarbon receptor. Biochem Biophys Res Commun 2002;291:1194–200.
[96] Quintana FJ, Basso AS, Iglesias AH, Korn T, Farez MF, Bettelli E, et al. Control of T(reg) and T(H)17 cell differentiation by the aryl hydrocarbon receptor. Nature 2008;453:65–71.
[97] van Grevenynghe J, Bernard M, Langouet S, Le Berre C, Fest T, Fardel O. Human CD34-positive hematopoietic stem cells constitute targets for carcinogenic polycyclic aromatic hydrocarbons. J Pharmacol Exp Ther 2005;314:693–702.
[98] Yamaguchi K, Near RI, Matulka RA, Shneider A, Toselli P, Trombino AF, et al. Activation of the aryl hydrocarbon receptor/transcription factor and bone marrow stromal cell-dependent preB cell apoptosis. J Immunol 1997;158:2165–73.
[99] Yoon BI, Li GX, Kitada K, Kawasaki Y, Igarashi K, Kodama Y, et al. Mechanisms of benzene-induced hematotoxicity and leukemogenicity: cDNA microarray analyses using mouse bone marrow tissue. Environ Health Perspect 2003;111:1411–20.
[100] Hirabayashi Y, Inoue T. Toxicogenomics applied to hematotoxicology. In: Borlak J, editor. Handbook of toxicogenomics. Weinheim: Wiley-VCH, Verlag GmbH; 2005. p. 583–608. Chapter 24.